ACS APPLIED MATERIALS & INTERFACES

Research Article

www.acsami.org

Synthesis and Characterization of Hydrazide-Linked and Amide-Linked Organic Polymers

Zhongshan Liu,[†,‡] Junjie Ou,[*,†] Hongwei Wang,[†] Xin You,[†,‡] and Mingliang Ye[*,†]

[†]Key Laboratory of Separation Science for Analytical Chemistry, Dalian Institute of Chemical Physics, Chinese Academy of Sciences, Dalian 116023, China

[‡]University of Chinese Academy of Sciences, Beijing 100049, China

Supporting Information

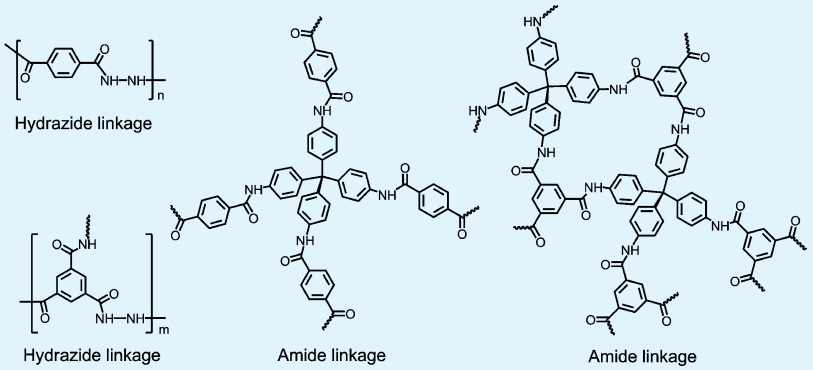

ABSTRACT: Four kinds of either hydrazide-linked or amide-linked polymers were facilely synthesized by using hydrazine, tetrakis(4-aminophenyl)methane (TAPM), terephthaloyl chloride (TPC), and trimesoyl chloride (TMC) as building blocks. The morphology, porosity, composition, and surface property of polymers were characterized by scanning electron microscopy, transmission electron microscopy, nitrogen adsorption−desorption measurement, ^{13}C/CP-MAS NMR, X-ray photoelectron spectroscopy, etc. The results indicated that building blocks had important effects on morphology and porosity. Poly(TMC−TAPM) synthesized with TMC and TAPM showed the highest surface area of 241.9 m^2 g^{-1}. In addition, note that a hollow structure with ∼20 nm wall thickness was formed in poly(TMC−hydrazine) prepared with TMC and hydrazine. Further study indicated that both carboxyl groups (−COOH) and hydrazide groups (−CONH−NH_2) existed on the surface of poly(TMC−hydrazine), besides the mainly hydrazide linkage (−CONH−NHOC−). Taking advantages of good hydrophilicity and special functional groups on the surface, we finally adopted poly(TMC−hydrazine) to enrich glycopeptides from tryptic digest via both hydrophilic interaction chromatography method with identification of 369 unique N-glycosylation sites and hydrazide chemistry method with identification of 88 unique N-glycosylation sites, respectively.

KEYWORDS: *hydrazide, amide, porous organic polymer, hollow structure, enrichment of glycopeptide*

1. INTRODUCTION

Porous organic polymers have continued to receive widespread research interest in the aspects of design, synthesis, and application. A wide range of options in organic monomers and synthesis strategies make it possible to design pore structures and specific properties for the organic polymers, which have been classified as hyper-cross-linked polymers (HCPs), conjugated microporous polymers (CMP), polymers of intrinsic microporosity (PIMs), and covalent organic frameworks (COFs), etc.[1−6] These porous organic polymers, which exhibited facile tuning on the pore size within microscale or mesoscale, have been widely applied in gas adsorption, gas separation, energy storage, catalyst supports, and chromatographic separation media.[1,7−13] Generally, rigid building blocks like conjugated aromatic compounds were required for construction of such porous organic polymers with persistent porosity.[14−17] However, the synthesis strategy would bring some limitations, such as hydrophobicity and difficulty to introduce specific functional groups, for most porous organic polymers. To address these drawbacks, researchers have attempted to introduce orthogonal functional groups into polymer skeleton for postmodification via Schiff base, click reaction, sulfonic reaction, and controlled/living radical polymerization.[18−22] It should be noted that more attention was paid to the design and synthesis of special functional monomers and the postmodification process in these approaches.

Amide bond and urea bond, which are known for their hydrophilicity, are prevalent linkages for synthesis of polymers. Particularly, aromatic polyamide has been widely exploited for

Received: September 12, 2016
Accepted: November 3, 2016
Published: November 3, 2016

DOI: 10.1021/acsami.6b11572
ACS Appl. Mater. Interfaces 2016, 8, 32060−32067

Scheme 1. (a) Chemical Structure of Building Blocks and (b) Probable Network of Polymers

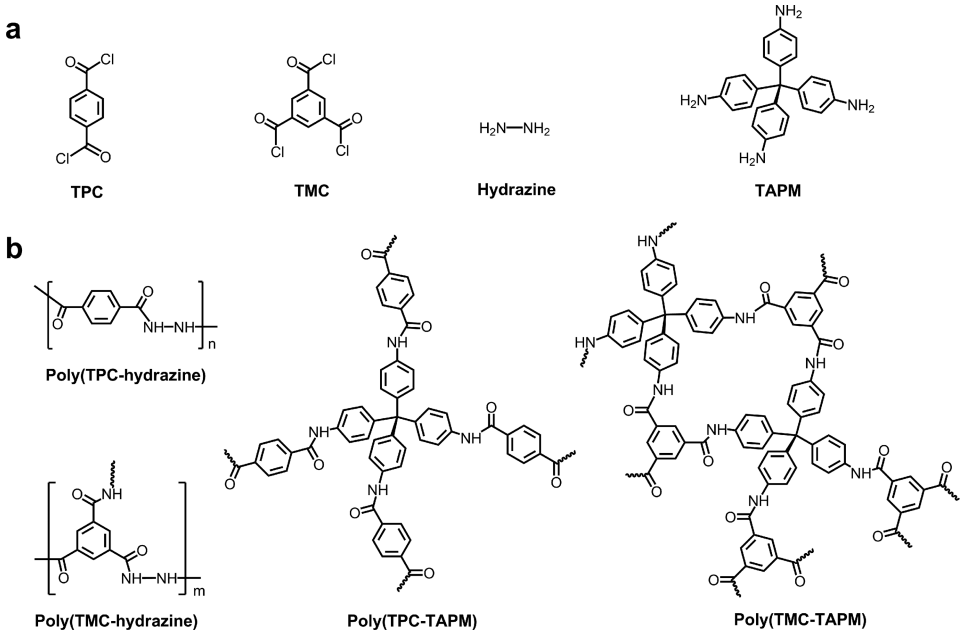

construction of thin film composite (TFC) membranes for water desalination.[23−25] Trimesoyl chloride (TMC) and *m*-phenylenediamine (MPD) were prevalent monomers for preparation of TFC membranes via interface polymerization. The water contact angle on such TFC membrane was less than 60°. The hydrophilicity could be attributed to the polar amide linkage (−CONH−) and residual functional groups.[26] Recently, such reactions have been adopted to fabricate three-dimensional porous organic polymers for applications in carbon dioxide capture, solid-phase extraction (SPE), and supports for catalysis.[27−31] For example, the organic polymer prepared by using TMC and *p*-phenylenediamine exhibited high thermal stability and good chemical stability.[29] Unfortunately, most such polymers usually showed very low surface area.

Herein, we prepared two kinds of hydrazide-linked polymers by using hydrazine, terephthaloyl chloride (TPC), and TMC as building blocks, as well as two kinds of amide-linked polymers by using tetrakis(4-aminophenyl)methane (TAPM), TPC, and TMC as building blocks (Scheme 1). The morphology and porosity were characterized by scanning electron microscopy (SEM), transmission electron microscopy (TEM), powder X-ray diffraction (PXRD), and nitrogen adsorption−desorption measurement. It was found that building blocks greatly affected the morphology and porosity of polymers. Taking poly(TMC−hydrazine) prepared with hydrazine and TMC as an example, we investigated its compositions and surface property by Fourier translation infrared spectrum (FT-IR), ^{13}C cross-polarization magnetic angle spinning (CP-MAS) NMR, elemental analysis, X-ray photoelectron spectroscopy (XPS), and zeta potential measurement, and finally applied it for enrichment of glycopeptides from tryptic digest via either HILIC or hydrazine chemistry methods.

2. EXPERIMENTAL SECTION

2.1. Chemicals and Materials. TPC (99%) was purchased from Tokyo Chemical Industry Co., LTD (Tokyo, Japan). TAPM (95%) was obtained from Shanghai Shaoyuan Co., Ltd. (Shanghai, China). Hydrazine solution (1.0 mol L^{-1} in THF), TMC (98%), triethylamine (99%), trifluoroacetic acid (TFA, 99%), formic acid (FA, 98%), and sodium periodate ($NaIO_4$) were obtained from Sigma-Aldrich (St. Louis, MO). 1,3,5-Benzenetricarbohydrazide was synthesized according to the reported method.[30] Tetrahydrofuran (THF) and acetic acid (AcOH) were purchased from Kemiou Chemical Regent Co., Ltd. (Tianjin, China) and dried prior to use. 4-Nitrobenzaldehyde (99%) was purchased from J&K Scientific Ltd. (Beijing, China). HPLC-grade acetonitrile (ACN) was obtained from Merck (Darmstadt, Germany). The water was doubly distilled and purified by Milli-Q system (Millipore Inc., Milford, MA). The C18 AQ beads (5 μm, 120 Å) were obtained from Michrom BioResources (Auburn, CA). The fused silica capillaries with inner diameter (i.d.) of 75 and 200 μm were purchased from Polymicro Technologies (Phoenix, AZ).

2.2. Preparation of Hydrazide-Linked Polymers. In a typical synthesis, the hydrazine solution (8.10 mL, 1.0 mol L^{-1} in THF), triethylamine (2.24 mL, 16.2 mmol), and THF (20 mL) were added into a 100 mL round-bottomed flask, which was equipped with a stirring bar and a 25 mL constant-pressure dropping funnel (CDF). The mixture of TPC (1.64 g, 8.1 mmol) and THF (5 mL) was added into the CDF. The solution in the flask was stirred in an ice−water bath when the TPC solution was added dropwise. After the reaction mixture was continuously stirred for 12 h at room temperature, the precipitate was separated by centrifugation, washed several times with water and ethanol, successively, and finally dried at 60 °C under vacuum, yielding powder that was denoted as poly(TPC−hydrazine) (65% yield). Similar to the above-mentioned steps, the poly(TMC−hydrazine) (70% yield) was prepared by replacing TPC with TMC (1.43 g, 5.4 mmol).

2.3. Preparation of Amide-Linked Polymers. For preparation of poly(TPC−TAPM), TAPM (114 mg, 0.3 mmol), triethylamine (166 μL, 1.2 mmol), and THF (12 mL) were added into a 25 mL round-bottomed flask, which was equipped with a stirring bar and a 25 mL of CDF. A mixture of TPC (122 mg, 0.6 mmol) and THF (3 mL) was added into the CDF. The solution in the flask was stirred in an ice−water bath when the TPC solution was added dropwise. After the reaction

DOI: 10.1021/acsami.6b11572
ACS Appl. Mater. Interfaces 2016, 8, 32060−32067

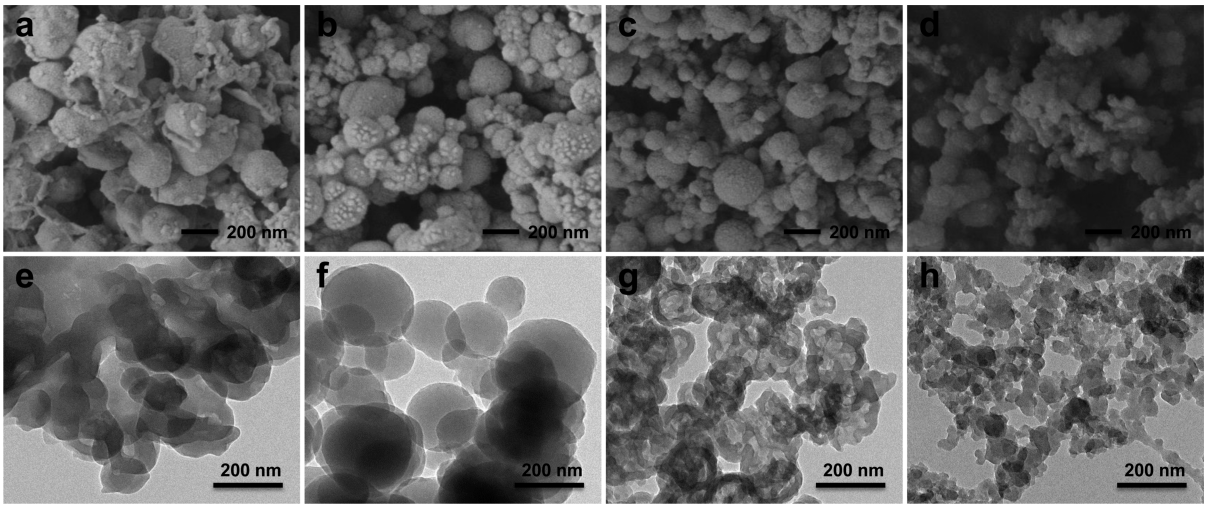

Figure 1. (a–d) SEM images and (e–h) TEM images of polymers. (a, e) Poly(TPC–hydrazine), (b, f) poly(TPC–TAPM), (c, g) poly(TMC–hydrazine), and (d, h) poly(TMC–TAPM). Magnification for SEM images is ×50 000.

mixture was continuously stirred for 12 h at room temperature, the precipitate was separated by centrifugation, washed several times with water, THF, and ethanol, successively, and finally dried at 60 °C under vacuum. The yield was 85%. Similarly, the monomer TPC was replaced with TMC (106 mg, 0.4 mmol) for preparation of poly(TMC-TAPM) (86% yield).

2.4. Characterization. The morphology study of polymers was carried out on SEM (GeminiSEM 300, Zeiss, Germany) and TEM (JEM-2100, JEOL Ltd., Tokyo, Japan). FT-IR spectra were obtained on a TENSOR 27 spectrometer with KBr pellets containing polymer sample (1.0 wt %, Bruker Optics, Germany). XPS data were acquired using an ESCALAB 250Xi XPS spectrometer with an Al Kα X-ray source (Thermo Scientific, U.S.A.). PXRD data were performed on an X'Pert Pro X-ray diffractometer with Cu Kα radiation (λ = 1.54 Å, PANalytical B.V., Holland). Solid-state ^{13}C/CP-MAS NMR spectra were recorded on a Bruker Advance III 500 NMR spectrometer. Elemental analysis was carried out on EMIA-8100H and EMG-930 (HORIBA, Japan). Nitrogen adsorption–desorption measurement was performed on a Quadrasorb SI surface area analyzer and pore size analyzer (Quantachrome Boynton Beach, U.S.A.). The samples were degassed at 120 °C under vacuum for 7 h prior to nitrogen adsorption–desorption measurement. The surface area was calculated via the Brunauer–Emmett–Teller (BET) method. The pore width was determined by the NLDFT model. The total porous volume was determined at P/P_0 = 0.98. The zeta potential of polymer in water (0.1 mg L^{-1}) was measured at 25 °C by a Zetasizer Nano ZS90 (Malvern Instruments Ltd., Malvern, U.K.). Water contact angles were measured on a DSA 100 machine (KRUSS, Hamburg, Germany) with 5 μL water drop after polymer powders were prepared into tablets under 3.5 MPa.

2.5. Quantification of Hydrazide Groups (–CONH–NH_2). The hydrazide density on the surface of poly(TMC–hydrazine) was measured according to the reported method (Figure S1).[32] Briefly, the stock solution was prepared by dissolving 4-nitrobenzaldehyde (10 mg) in 45 mL of anhydrous methanol containing 0.8% (v/v) AcOH. After equilibration with 0.8% AcOH/methanol solution, the polymer powder (3 mg) was dispersed in 1 mL stock solution to react for 4 h with gentle oscillation. The polymer was then isolated by centrifugation and washed twice by 0.8% AcOH/methanol (1 mL). All supernatants were collected, and the concentration of residual 4-nitrobenzaldehyde was measured at 264 nm by UV–vis spectroscopy (V550, JASCO, Japan). The hydrazide density was determined by the following equation

$$\text{hydrazide density} = \frac{C_0V_0 - C_sV_s}{m}$$

where C_0 is the pristine concentration of 4-nitrobenzaldehyde in stock solution, V_0 is the volume of reaction solution, C_s is the residual concentration of 4-nitrobenzaldehyde in supernatant, V_s is the volume of supernatant, and m is the weight of poly(TMC–hydrazine).

2.6. Application of Polymer for Enrichment of Glycopeptides. Taking advantages of good hydrophilicity and residual hydrazide groups, the poly(TMC–hydrazine) was used for enrichment of glycopeptides by HILIC and hydrazide chemistry methods, respectively. The tryptic digest was prepared to evaluate poly(TMC–hydrazine) according to the reported method.[33] The HILIC method was carried out by the following protocol. Briefly, the powder of poly(TMC–hydrazine) was first equilibrated with a loading solution (ACN/H_2O/TFA, 88/11.9/0.1, v/v/v) three times and then added into a solution of protein tryptic digest (dissolved in 400 μL of loading solution). The mixture was incubated for 30 min with gentle oscillation at room temperature. Then the polymer was isolated by centrifugation and rinsed with the loading solution (3 × 200 μL). Finally, the captured glycopeptides were eluted with a solution of ACN/H_2O/TFA (40 μL, 30/69.9/0.1, v/v/v) for 10 min shaking powerfully. Part of the eluate was directly analyzed by MALDI-TOF MS, while another part was dried and redissolved in aqueous solution of ammonium bicarbonate (10 mmol L^{-1}) for deglycosylation with PNGase F at 37 °C and cLC-MS/MS analysis. The methods for MALDI-TOF MS and cLC-MS/MS are described in the Supporting Information.

For the hydrazide chemistry method, the dry tryptic peptides were dissolved in oxidation buffer (0.32 mL, 100 mmol L^{-1} NaAc, 150 mmol L^{-1} NaCl, pH = 5.5), into which the $NaIO_4$ solution (0.08 mL, 50 mmol L^{-1}) was added. The reaction was kept in the dark with constant shaking at room temperature for 1 h and quenched by adding sodium thiosulfate solution (0.08

DOI: 10.1021/acsami.6b11572
ACS Appl. Mater. Interfaces 2016, 8, 32060–32067

mL, 100 mmol L^{-1}). After such reactions, pristine glycopeptides in tryptic digest were converted into oxidized glycopeptides containing aldehyde groups. Poly(TMC−hydrazine) (5 mg) was added into above-mentioned reaction mixture and incubated for 12 h at room temperature to capture the oxidized glycopeptides by formation of Schiff base (−CONH−N=C−) between aldehyde group and hydrazide group (−CONH−NH_2) on the surface of the polymer. Then the polymer was isolated by centrifugation and rinsed with NaCl solution (1.5 mol L^{-1}, 3 × 200 μL), methanol (3 × 200 μL), and aqueous solution of ammonium bicarbonate (100 mmol L^{-1}, 3 × 200 μL), successively. The glycopeptides on the polymer were selectively released by incubating the polymer with a solution of ammonium bicarbonate (10 mmol L^{-1}) containing PNGase F for 12 h at 37 °C. The deglycosylated peptides were carefully collected for MALDI-TOF MS or cLC-MS/MS analysis.

3. RESULTS AND DISCUSSION

3.1. Synthesis, Morphology, and Porosity of Polymers. To investigate the effects of building blocks on morphology and porosity, the monomers containing two kinds of acyl chlorides (TPC and TMC), hydrazine and TAPM with rigid geometry, were selected for synthesis of polymers. The chemical structures of monomers and probable network of four kinds of polymers are shown in Scheme 1. Among them, poly(TPC−hydrazine) was linear polymer in theory. Other three polymers should show cross-linked network. The molar ratio of two kinds of reacting functional groups was set at 1:1 for all polymers.

The SEM images shown in Figure 1 indicated that four polymers tended to form spheroidal particles due to their immiscibility, and some particles further aggregated with each other, leading to an irregular morphology. Although poly(TPC−hydrazine) was linear polymer, it was insolvable in the solvents like THF, water, and ethanol. The poly(TPC−hydrazine) particles exhibited relative good dispersity, of which the diameters were mainly smaller than 200 nm (Figure 1a). For cross-linked poly(TPC−TAPM), most of the particles became more irregular and smaller (Figure 1b). Such phenomenon was possibly related to the rapid phase separation due to its higher cross-linking degree than that of linear poly(TPC−hydrazine), which also happened in the formation of poly(TMC−hydrazine) and poly(TMC−TAPM) (Figure 1c−d). To achieve more features of morphology, these polymers were further characterized by TEM (Figure 1e−h). The sizes of particles were in accordance with the results obtained by SEM images. Obvious macropores could not be observed in poly(TPC−hydrazine) and poly(TPC−TAPM). It was worth noting that a hollow structure was formed in poly(TMC−hydrazine) (Figure 1g and Figure S2). The inner diameters of hollow particles ranged from a few tens of nanometers to more than 100 nanometers. The wall thickness of hollow particles was mainly about 20 nm, which facilitated a stable structure.

The four polymers were then characterized by PXRD as shown in Figure S3. Three strong peaks were observed at 2θ = 18.3°, 22.4°, and 22.4°, respectively, for linear poly(TPC−hydrazine). For other three cross-linked polymers, only broadening peaks were observed, suggesting that these polymers were amorphous. The results were acceptable because it was difficult to obtain ideal cross-linking structure and efficient packing via π−π interactions between aromatic phenyl units, which was prevalent in COFs with high crystallinity.[34−36]

The porosities of three cross-linked polymers were determined by nitrogen adsorption−desorption measurement (Figure 2a). Based on the BET model, the total surface area was

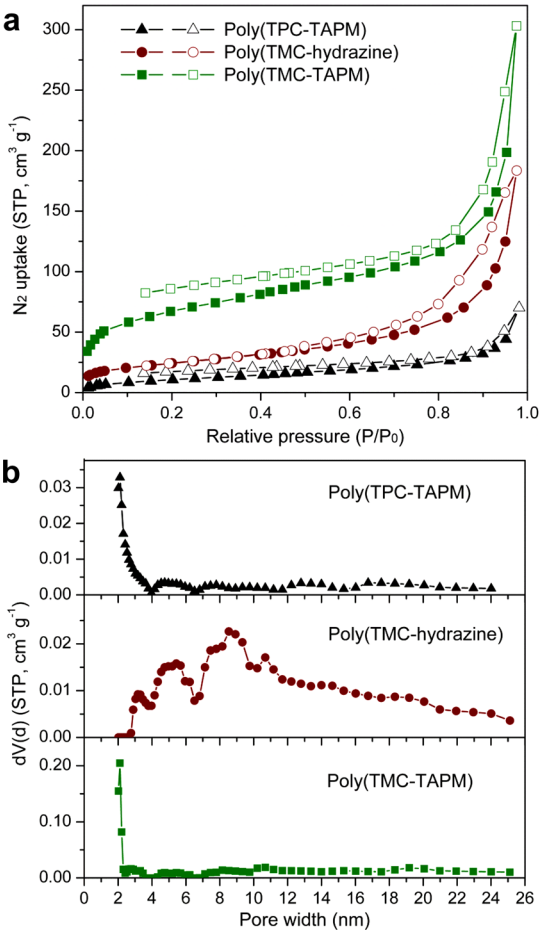

Figure 2. (a) Nitrogen adsorption−desorption isotherm of polymers and (b) pore width determined by NLDFT model with adsorption isotherm.

calculated to be 41.3, 87.1, and 241.9 m^2 g^{-1} for poly(TPC−TAPM), poly(TMC−hydrazine), and poly(TMC−TAPM), respectively. Then the nitrogen adsorption data ($0.2 < P/P_0 < 0.5$) were further analyzed by the *t*-plot method (Figure S4). It was found that there were not any micropores (diameter less than 2 nm) in poly(TPC−TAPM) and poly(TMC−hydrazine). However, the micropore surface area was 89.7 m^2 g^{-1} for poly(TMC−TAPM), indicating the formation of micropore structure. The results suggested rigid linkage and high cross-linking degree were very helpful to form persistent porosity. Through the NLDFT model, the pore widths were obtained as shown in Figure 2b. Poly(TPC−TAPM) and poly(TMC−TAPM), which were formed via amide linkages, showed the similar mesopore size of ∼2.1 nm. Note that poly(TMC−hydrazine) demonstrated a very broad pore width distribution, ranging from 3 to 25 nm, which should be attributed to the hollow structure with different inner diameter. The total pore volume of poly(TMC−hydrazine) reached up to 0.28 cm^3 g^{-1}.

3.2. Composition Analysis and Surface Property. The compositions of four polymers were characterized by FT-IR, As shown in Figure 3a, a strong absorption peak at 1655 cm^{-1} corresponding to stretching vibration of C=O bond was

DOI: 10.1021/acsami.6b11572
ACS Appl. Mater. Interfaces 2016, 8, 32060−32067

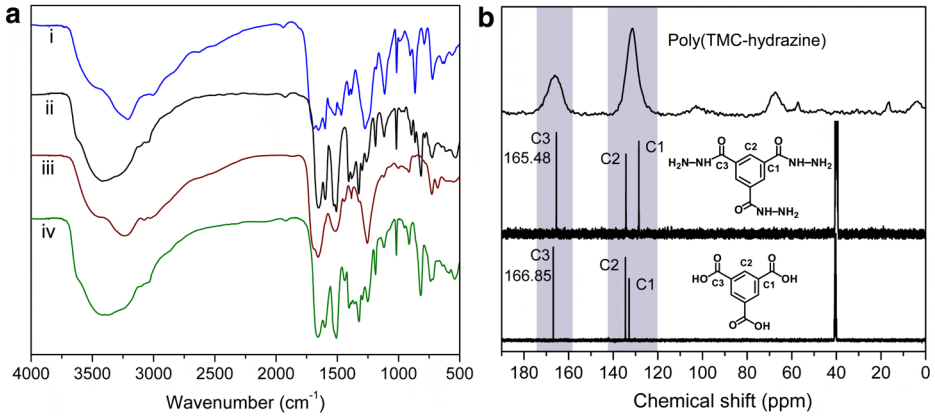

Figure 3. (a) FT-IR spectra of polymers. i, poly(TPC−hydrazine); ii, poly(TPC−TAPM); iii, poly(TMC−hydrazine); iv, poly(TMC−TAPM). (b) ^{13}C NMR spectra of trimesitinic acid, 1,3,5-benzenetricarbohydrazide, and poly(TMC−hydrazine).

clearly observed for all polymers, suggesting the formation hydrazide linkage or amide linkage, since the adsorption peak for C═O in the acyl chlorides usually located at about 1760 cm^{-1}. The peak at 1258 cm^{-1} arose from the stretching vibration of C−N bond. The peak at 1520 cm^{-1} corresponded to the bending vibration of N−H bond, and the absorption bands at 3230 and 3500 cm^{-1} were ascribed to the stretching vibrations of N−H bond.

The surface property of polymers was then investigated by water contact angle (Figure S5). Both hydrazide-linked and amide-linked polymers exhibited good hydrophilicity according to the water contact angles ranging from 21.8° to 46.6°. It was noted that two amide-linked polymers showed better hydrophilicity than two hydrazide-linked polymers. Especially for poly(TMC−TAPM), the good hydrophilicity and above-mentioned relative large surface area made such polymer very promising for application in aqueous medium as adsorbents and catalyst supports.

Apart from the mainly hydrazide and amide linkages, we were also interested in the residual functional groups, such as hydrazide group (−CONH−NH_2), amine group (−NH_2), and carboxyl group (−COOH), which usually have important effects on hydrophilicity and have potential to provide special interaction sites for target molecules. However, such residual functional groups were difficult to identify from FT-IR data. Herein, we took poly(TMC−hydrazine) as an example and used solid ^{13}C/CP-MAS NMR, elemental analysis, XPS, and zeta potential measurement to further study the functional groups in polymer. Prior to ^{13}C/CP-MAS NMR analysis, we compared the ^{13}C NMR spectra of 1,3,5-benzenetricarbohydrazide and trimesitinic acid. As shown in Figure 3b, the carbon atom denoted by C2 was determined according to the distortionless enhancement by polarization transfer (DEPT) spectrum. After the carboxyl groups were converted into hydrazide groups, the chemical shift of C1 changed from 132.91 to 128.51 ppm. Therefore, the broadening peak at 131.45 ppm in ^{13}C/CP-MAS NMR spectrum for poly(TMC−hydrazine) should belong to the carbon atoms in benzene ring. Another broadening peak at 166.19 ppm was assigned to the carbon atom in C═O bond according to the chemical shift of carbon atoms denoted by C3 in spectra of 1,3,5-benzenetricarbohydrazide and trimesitinic acid. Due to being very close in chemical shift, it was still difficult to distinguish the peaks between carboxyl groups and hydrazide-based linkage groups. Then the contents of carbon, nitrogen, hydrogen, and oxygen in poly(TMC−hydrazine) were determined by elemental analysis. Comparing with theoretical values (C, 52.94%; H, 2.94%; O, 23.53%; N, 20.95%, wt %) calculated with $(C_9H_6N_3O_3)_n$, the content of carbon (44.25%) was relative low, while the contents of both hydrogen (3.77%) and oxygen (27.42) were higher. The mass ratio of hydrogen to carbon was calculated to be 1:11.7, and higher than the theoretical value of 1:18.0. Similarly, the mass ratio of oxygen to carbon was 1:1.6, and higher than the theoretical value of 1:2.2. It was deduced such deviations were likely related to the unreacted functional groups in monomers.

The full XPS spectrum of poly(TMC−hydrazine) is shown in Figure 4a and indicated that the polymer was mainly

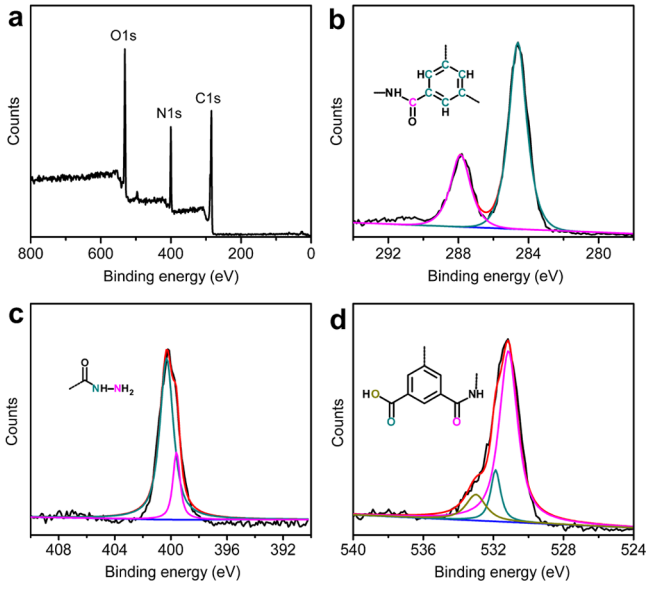

Figure 4. (a) XPS spectra of poly(TMC−hydrazine) and high-resolution spectra of (b) C 1s, (c) N 1s, and (d) O 1s. Other curves in (b−d): black, raw data; red, fitted data; blue, baseline.

composed of carbon, nitrogen, and oxygen. In high-resolution C 1s spectrum (Figure 4b), the major peaks at 284.61 and 287.88 eV were assigned to the carbon atoms in benzene ring (C−H, C−C, and C═C) and hydrazide-based linkage groups (−CONH−NHOC−), respectively. In Figure 4c, the major peak at 400.30 eV was assigned to the binding energies of linkage groups (−CONH−NHOC−), while a minor peak at

DOI: 10.1021/acsami.6b11572
ACS Appl. Mater. Interfaces 2016, 8, 32060−32067

399.60 eV should correspond to the hydrazide groups (−CONH−*NH_2). The nitrogen atom arising from hydrazide groups was calculated to be 18.1% in proportion to total nitrogen atoms (Table S1). For the oxygen atom, high-resolution O 1s spectrum (Figure 4d) was well fitted by using three components at 531.14 eV (−CONH−NHOC−), 531.87 eV (-C*OOH), and 533.00 eV (−CO*OH), respectively. The ratio of hydrazide-based linkage groups to carboxyl groups ([−CONH−NHOC−]:[−COOH]) was about 2.5:1 on the surface of polymer. As a result, we concluded that a few hydrazide groups and carboxyl groups generated by hydrolysis of acyl chloride groups should be concurrently exposed on the surface of polymers.

Further attention was paid to the quantification of residual hydrazide groups (−CONH−NH_2) on the surface of poly(TMC−hydrazine). The quantification method was based on the reaction of 4-nitrobenzaldehyde with hydrazide groups (Figure S1). The density of hydrazide groups was calculated to be 0.42 mmol g^{-1}, indicating the existence of hydrazide groups on the surface of poly(TMC−hydrazine). Through the same measurement method, the reported magnetic particles (Fe_3O_4@SiO_2), which were modified with 3-glycidoxypropyltrimethoysilane and hydrazine hydrate, showed hydrazine density of 0.947 mmol g^{-1}.[32] Though the hydrazide density in the present work was not as high as the reported result, the synthesis approach of polymer was very facile, time-saving, and cost-effective.

Furthermore, if both hydrazide groups and carboxyl groups existed concurrently, the net charge on the surface of poly(TMC−hydrazine) should be adjusted by the pH. Therefore, we prepared a series of aqueous suspensions of poly(TMC−hydrazine) (0.1 mg mL^{-1}), of which the pH values were adjusted by HCl or NaOH solution. As shown in Figure 5,

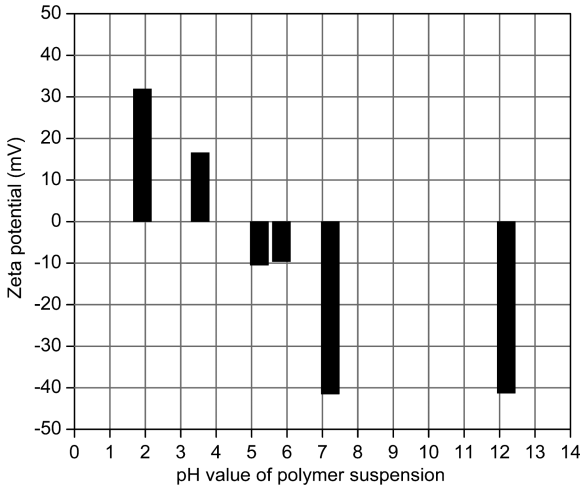

Figure 5. Dependence of zeta potential on poly(TMC−hydrazine) suspensions with different pH values.

the values of zeta potential were positive at pH lower than 4, resulting from the protonation of hydrazine group (−CONH−NH_3^+). At pH higher than 5, the surface of polymer demonstrated negative charge, which was attributed to the ionized carboxyl groups (−COO^-). The result indicated a zwitterionic feature for the surface of poly(TMC−hydrazine).

3.3. Application of poly(TMC−hydrazine) for Enrichment of Glycopeptides. In shotgun proteomics, selective enrichment of glycopeptides from complex protein digest has been a critical prerequisite for in-depth glycosylation research due to their relative low abundance and low ionization.[37] Among enrichment protocols, both HILIC and hydrazide chemistry methods have achieved more attention because of their unique advantages, which compensated for the deficiency of other methods like boronic acid chemistry and lectin affinity chromatography.[38−42] Particularly, the materials like silica particles and monolithic column grafted with zwitterionic organic moieties, such as cysteine (Cys), glutathione (GSH), and [2-(methacryloyloxy)ethyl]dimethyl-(3-sulfopropyl) ammonium hydroxide (MSA), were very popular for enrichment of glycopeptides via HILIC mode.[33,38,43,44]

The poly(TMC−hydrazine) not only showed good hydrophilicity but also exhibited zwitterionic surface structure due to the hydrazide linkage and residual functional groups. Therefore, we attempted to apply poly(TMC−hydrazine) to enrich glycopeptides from IgG digest via HILIC method (Figure 6a). Twenty glycopeptides were clearly detected in MALDI-TOF mass spectrum (signal-to-noise ratios, $S/N > 20$) (Figure 6c). For hydrazide chemistry method, the glycopeptides in tryptic digest were first oxidized by $NaIO_4$ to generate aldehyde groups, which then reacted with hydrazide groups (−CONH−NH_2) on polymer surface (Figure 6b). The formation of Schiff base (−CONH−N═C−) made the oxidized glycopeptide especially be enriched by poly(TMC−hydrazine). After washing several times to remove nonglycopeptides, the deglycosylated peptides were selectively released from poly(TMC−hydrazine) with PNGase F and identified by MALDI-TOF MS with m/z of 1158.68 and 1190.50 (Figure 6d).

Besides simple IgG digest, we further adopted poly(TMC−hydrazine) to enrich glycopeptides in tryptic digest of HeLa cell proteins. Through the HILIC method, a total of 369 unique N-glycosylation sites were identified in 80 μg of tryptic digest by three independent LC-MS/MS analyses (Figure 6e). As for hydrazide chemistry method, we carried out the enrichment process in buffer solution with pH = 5.5. However, the result in Figure 6f showed that only a total of 42 unique N-glycosylation sites were identified in 80 μg tryptic digest. Generally, the reaction of hydrazide group with aldehyde group is reversible. Weak acid condition would promote such reaction to form Schiff base. The buffer solution with pH = 5.5 was an optimal condition for hydrazide-modified materials. In the present work, the carboxyl groups on polymer surface possibly affected the reactivity of hydrazide groups, even decreasing the enrichment efficiency. In buffer solution with pH = 5.5, the zeta potential was −15.2 mV for poly(TMC−hydrazine), indicating carboxyl groups were ionized. The pH of buffer solution was increased to 3.3, and the surface net charge on polymer surface seemed to be positive according to zeta potential measurement (Figure 5). As shown in Figure 6g, the identified unique N-glycosylation sites were increased by 110% in buffer solution with pH = 3.3.

4. CONCLUSIONS

We have demonstrated a facile method for synthesis of hydrazide-linked and amide-linked organic polymers by using four building blocks with different geometries. The building blocks greatly affected the morphology, porosity, and surface property of polymers. As expected, rigid building blocks and high cross-linking degree would generate persistent porosity and facilitate surface area. In addition, the four polymers exhibited very good hydrophilicity that was attributed to the hydrazide and amide linkages, as well as residual functional

DOI: 10.1021/acsami.6b11572
ACS Appl. Mater. Interfaces 2016, 8, 32060−32067

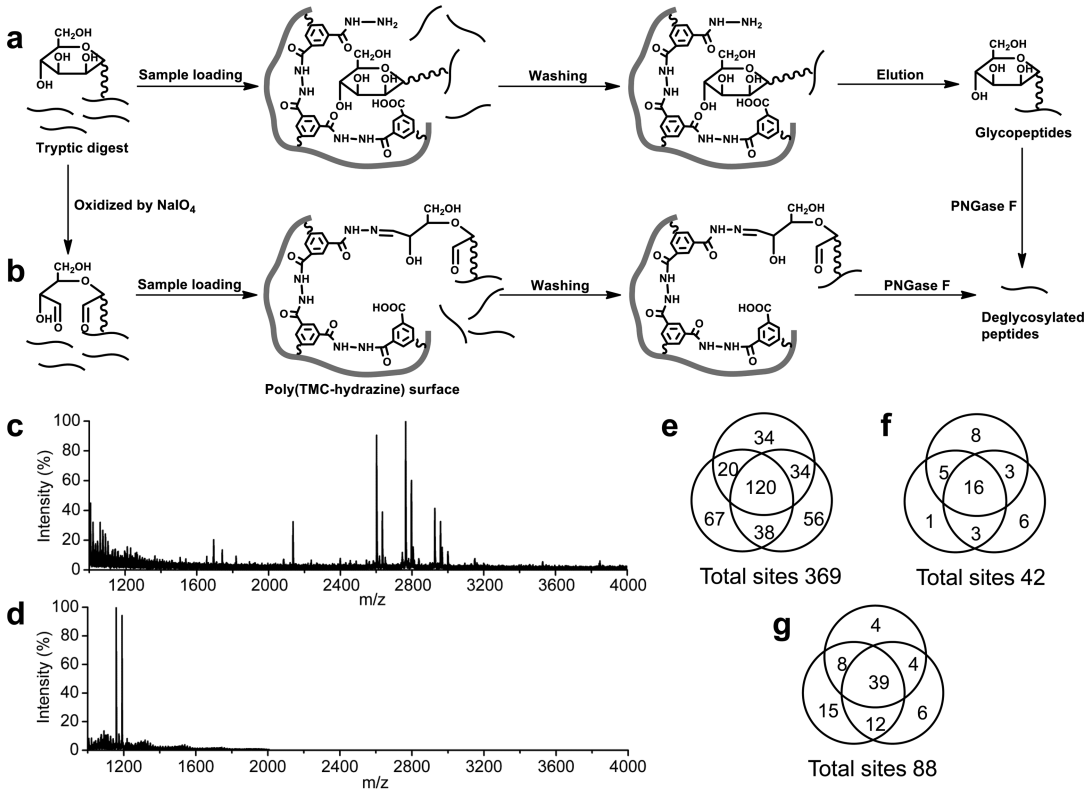

Figure 6. Application of poly(TMC−hydrazine) for enrichment of glycopeptides. Schematic enrichment steps for (a) HILIC and (b) hydrazide chemistry methods. MALDI-TOF spectra of glycopeptides in IgG digest enriched by (c) HILIC and (d) hydrazide chemistry methods. (e−g) Overlap and total number of unique N-glycosylation sites identified in 80 μg tryptic digest of HeLa cell proteins with three one-dimensional LC-MS/MS analyses. Enrichment conditions: (e) HILIC method, (f) hydrazide chemistry at pH = 5.5, and (g) hydrazide chemistry at pH = 3.3.

groups generated from starting monomers. Though the surface area of polymers in the present work was not as large as that of other polymers (COFs, CMPs, and PIMs, etc.), the hydrazide and amide linkages could provide many kinds of interactions, which made such polymers very promising for application in adsorbents and metal catalyst supports. It was worth noting that a stable hollow structure was directly formed in poly(TMC−hydrazine) without templates and other additives. Considering its remarkable features and properties, we would like to tune particle size distribution and wall thickness, as well as exploit its application in our future work.

■ ASSOCIATED CONTENT

Supporting Information

. The Supporting Information is available free of charge on the ACS Publications website at DOI: 10.1021/acsami.6b11572.

Methods for MALDI-TOF MS and cLC-MS/MS analyses; quantification mechanism for hydrazide groups; more TEM images of poly(TMC−hydrazine); PXRD patterns; *t*-plot analyses for N_2 adsorption data at $0.2 < P/P_0 < 0.5$; water contact angle and summary of compositions obtained from XPS spectra (PDF)

■ AUTHOR INFORMATION

Corresponding Authors

*E-mail: junjieou@dicp.ac.cn. Tel.: +86-411-84379576.
*E-mail: mingliang@dicp.ac.cn. Tel.: +86-411-84379520.

Notes

The authors declare no competing financial interest.

■ ACKNOWLEDGMENTS

Financial support is gratefully acknowledged from the China State Key Basic Research Program Grant (2012CB910601), National Natural Sciences Foundation of China (No. 21535008), and the China State Key Research Grant (2016YFA0501402) to M.Y. as well as the National Natural Sciences Foundation of China (No. 21575141) to J.O.

■ REFERENCES

(1) Wood, C. D.; Tan, B.; Trewin, A.; Niu, H.; Bradshaw, D.; Rosseinsky, M. J.; Khimyak, Y. Z.; Campbell, N. L.; Kirk, R.; Stöckel, E.; Cooper, A. I. Hydrogen Storage in Microporous Hypercrosslinked Organic Polymer Networks. *Chem. Mater.* **2007**, *19*, 2034−2048.

(2) Ratvijitvech, T.; Barrow, M.; Cooper, A. I.; Adams, D. J. The Effect of Molecular Weight on the Porosity of Hypercrosslinked Polystyrene. *Polym. Chem.* **2015**, *6*, 7280−7285.

(3) Jiang, J.; Su, F.; Trewin, A.; Wood, C. D.; Campbell, N. L.; Niu, H.; Dickinson, C.; Ganin, A. Y.; Rosseinsky, M. J.; Khimyak, Y. Z.; Cooper, A. I. Conjugated Microporous Poly(aryleneethynylene) Networks. *Angew. Chem., Int. Ed.* **2007**, *46*, 8574−8578.

(4) Maffei, A. V.; Budd, P. M.; McKeown, N. B. Adsorption Studies of a Microporous Phthalocyanine Network Polymer. *Langmuir* **2006**, *22*, 4225−4229.

(5) McKeown, N. B.; Budd, P. M. Polymers of Intrinsic Microporosity (PIMs): Organic Materials for Membrane Separations, Heterogeneous Catalysis, and Hydrogen Storage. *Chem. Soc. Rev.* **2006**, *35*, 675−683.

(6) Ding, S.; Wang, W. Covalent Organic Frameworks (COFs): From Design to Applications. *Chem. Soc. Rev.* **2013**, *42*, 548−568.

(7) Feng, X.; Ding, X.; Jiang, D. Covalent Organic Frameworks. *Chem. Soc. Rev.* **2012**, *41*, 6010−6022.

DOI: 10.1021/acsami.6b11572
ACS Appl. Mater. Interfaces 2016, 8, 32060−32067

(8) Zeng, Y.; Zou, R.; Zhao, Y. Covalent Organic Frameworks for CO_2 Capture. *Adv. Mater.* **2016**, *28*, 2855−2873.
(9) Kaur, P.; Hupp, J. T.; Nguyen, S. T. Porous Organic Polymers in Catalysis: Opportunities and Challenges. *ACS Catal.* **2011**, *1*, 819−835.
(10) Mondal, J.; Trinh, Q. T.; Jana, A.; Ng, W. K. H.; Borah, P.; Hirao, H.; Zhao, Y. Size-Dependent Catalytic Activity of Palladium Nanoparticles Fabricated in Porous Organic Polymers for Alkene Hydrogenation at Room Temperature. *ACS Appl. Mater. Interfaces* **2016**, *8*, 15307−15319.
(11) Lu, C.; Liu, S.; Xu, J.; Ding, Y.; Ouyang, G. Exploitation of a Microporous Organic Polymer as a Stationary Phase for Capillary Gas Chromatography. *Anal. Chim. Acta* **2016**, *902*, 205−211.
(12) Yang, C.; Liu, C.; Cao, Y.; Yan, X. Facile Room-Temperature Solution-Phase Synthesis of a Spherical Covalent Organic Framework for High-Resolution Chromatographic Separation. *Chem. Commun.* **2015**, *51*, 12254−12257.
(13) Qian, H.; Yang, C.; Yan, X. Bottom-up Synthesis of Chiral Covalent Organic Frameworks and Their Bound Capillaries for Chiral Separation. *Nat. Commun.* **2016**, *7*, 12104.
(14) McKeown, N. B.; Budd, P. M.; Msayib, K. J.; Ghanem, B. S.; Kingston, H. J.; Tattershall, C. E.; Makhseed, S.; Reynolds, K. J.; Fritsch, D. Polymers of Intrinsic Microporosity (PIMs): Bridging the Void between Microporous and Polymeric Materials. *Chem. - Eur. J.* **2005**, *11*, 2610−2620.
(15) Shultz, A. M.; Farha, O. K.; Hupp, J. T.; Nguyen, S. T. Synthesis of Catalytically Active Porous Organic Polymers from Metalloporphyrin Building Blocks. *Chem. Sci.* **2011**, *2*, 686−689.
(16) Pandey, P.; Farha, O. K.; Spokoyny, A. M.; Mirkin, C. A.; Kanatzidis, M. G.; Hupp, J. T.; Nguyen, S. T. A "Click-Based" Porous Organic Polymer from Tetrahedral Building Blocks. *J. Mater. Chem.* **2011**, *21*, 1700−1703.
(17) Holst, J. R.; Stöckel, E.; Adams, D. J.; Cooper, A. I. High Surface Area Networks from Tetrahedral Monomers: Metal-Catalyzed Coupling, Thermal Polymerization, and "Click" Chemistry. *Macromolecules* **2010**, *43*, 8531−8538.
(18) Guillerm, V.; Weselinski, L. J.; Alkordi, M.; Mohideen, M. I. H.; Belmabkhout, Y.; Cairns, A. J.; Eddaoudi, M. Porous Organic Polymers with Anchored Aldehydes: A New Platform for Post-Synthetic Amine Functionalization en Route for Enhanced CO_2 Adsorption Properties. *Chem. Commun.* **2014**, *50*, 1937−1940.
(19) Nagai, A.; Guo, Z.; Feng, X.; Jin, S.; Chen, X.; Ding, X.; Jiang, D. Pore Surface Engineering in Covalent Organic Frameworks. *Nat. Commun.* **2011**, *2*, 536.
(20) Li, B.; Su, F.; Luo, H.; Liang, L.; Tan, B. Hypercrosslinked Microporous Polymer Networks for Effective Removal of Toxic Metal Ions from Water. *Microporous Mesoporous Mater.* **2011**, *138*, 207−214.
(21) Lv, Y.; Lin, Z.; Svec, F. Hypercrosslinked Large Surface Area Porous Polymer Monoliths for Hydrophilic Interaction Liquid Chromatography of Small Molecules Featuring Zwitterionic Functionalities Attached to Gold Nanoparticles Held in Layered Structure. *Anal. Chem.* **2012**, *84*, 8457−8460.
(22) Mai, W.; Sun, B.; Chen, L.; Xu, F.; Liu, H.; Liang, Y.; Fu, R.; Wu, D.; Matyjaszewski, K. Water-Dispersible, Responsive, and Carbonizable Hairy Microporous Polymeric Nanospheres. *J. Am. Chem. Soc.* **2015**, *137*, 13256−13259.
(23) Elimelech, M.; Phillip, W. A. The Future of Seawater Desalination: Energy, Technology, and the Environment. *Science* **2011**, *333*, 712−717.
(24) Lau, W. J.; Gray, S.; Matsuura, T.; Emadzadeh, D.; Paul Chen, J.; Ismail, A. F. A Review on Polyamide Thin Film Nanocomposite (TFN) Membranes: History, Applications, Challenges, and Approaches. *Water Res.* **2015**, *80*, 306−324.
(25) Gao, Y.; de Jubera, A. M. S.; Mariñas, B. J.; Moore, J. S. Nanofiltration Membranes with Modified Active Layer Using Aromatic Polyamide Dendrimers. *Adv. Funct. Mater.* **2013**, *23*, 598−607.
(26) Karan, S.; Jiang, Z.; Livingston, A. G. Sub−10 nm Polyamide Nanofilms with Ultrafast Solvent Transport for Molecular Separation. *Science* **2015**, *348*, 1347−1351.
(27) Qian, H.; Zheng, J.; Zhang, S. Preparation of Microporous Polyamide Networks for Carbon Dioxide Capture and Nanofiltration. *Polymer* **2013**, *54*, 557−564.
(28) Zulfiqar, S.; Sarwar, M. I.; Yavuz, C. T. Melamine Based Porous Organic Amide Polymers for CO_2 Capture. *RSC Adv.* **2014**, *4*, 52263−52269.
(29) Suresh, V. M.; Bonakala, S.; Atreya, H. S.; Balasubramanian, S.; Maji, T. K. Amide Functionalized Microporous Organic Polymer (AmMOP) for Selective CO_2 Sorption and Catalysis. *ACS Appl. Mater. Interfaces* **2014**, *6*, 4630−4637.
(30) Zhang, C.; Li, G.; Zhang, Z. A Hydrazone Covalent Organic Polymer Based Micro-Solid Phase Extraction for Online Analysis of Trace Sudan Dyes in Food Samples. *J. Chromatogr. A* **2015**, *1419*, 1−9.
(31) Li, L.; Chen, Z.; Zhong, H.; Wang, R. Urea-Based Porous Organic Frameworks: Effective Supports for Catalysis in Neat Water. *Chem. - Eur. J.* **2014**, *20*, 3050−3060.
(32) Huang, G.; Sun, Z.; Qin, H.; Zhao, L.; Xiong, Z.; Peng, X.; Ou, J.; Zou, H. Preparation of Hydrazine Functionalized Polymer Brushes Hybrid Magnetic Nanoparticles for Highly Specific Enrichment of Glycopeptides. *Analyst* **2014**, *139*, 2199−2206.
(33) Liu, J.; Wang, F.; Lin, H.; Zhu, J.; Bian, Y.; Cheng, K.; Zou, H. Monolithic Capillary Column Based Glycoproteomic Reactor for High-Sensitive Analysis of N-Glycoproteome. *Anal. Chem.* **2013**, *85*, 2847−2852.
(34) Fang, Q.; Wang, J.; Gu, S.; Kaspar, R. B.; Zhuang, Z.; Zheng, J.; Guo, H.; Qiu, S.; Yan, Y. 3D Porous Crystalline Polyimide Covalent Organic Frameworks for Drug Delivery. *J. Am. Chem. Soc.* **2015**, *137*, 8352−8355.
(35) Farha, O. K.; Spokoyny, A. M.; Hauser, B. G.; Bae, Y.-S.; Brown, S. E.; Snurr, R. Q.; Mirkin, C. A.; Hupp, J. T. Synthesis, Properties, and Gas Separation Studies of a Robust Diimide-Based Microporous Organic Polymer. *Chem. Mater.* **2009**, *21*, 3033−3035.
(36) Farha, O. K.; Bae, Y.-S.; Hauser, B. G.; Spokoyny, A. M.; Snurr, R. Q.; Mirkin, C. A.; Hupp, J. T. Chemical Reduction of a Diimide Based Porous Polymer for Selective Uptake of Carbon Dioxide versus Methane. *Chem. Commun.* **2010**, *46*, 1056−1058.
(37) Zhang, Y.; Zhang, C.; Jiang, H.; Yang, P.; Lu, H. Fishing the PTM Proteome with Chemical Approaches Using Functional Solid Phases. *Chem. Soc. Rev.* **2015**, *44*, 8260−8287.
(38) Shen, A.; Guo, Z.; Yu, L.; Cao, L.; Liang, X. A Novel Zwitterionic HILIC Stationary Phase Based on "Thiol-Ene" Click Chemistry between Cysteine and Vinyl Silica. *Chem. Commun.* **2011**, *47*, 4550−4552.
(39) Xiong, Z.; Qin, H.; Wan, H.; Huang, G.; Zhang, Z.; Dong, J.; Zhang, L.; Zhang, W.; Zou, H. Layer-by-Layer Assembly of Multilayer Polysaccharide Coated Magnetic Nanoparticles for the Selective Enrichment of Glycopeptides. *Chem. Commun.* **2013**, *49*, 9284−9286.
(40) Tian, Y.; Zhou, Y.; Elliott, S.; Aebersold, R.; Zhang, H. Solid-Phase Extraction of N-Linked Glycopeptides. *Nat. Protoc.* **2007**, *2*, 334−339.
(41) Chen, J.; Shah, P.; Zhang, H. Solid Phase Extraction of N-Linked Glycopeptides Using Hydrazide Tip. *Anal. Chem.* **2013**, *85*, 10670−10674.
(42) He, X.; Zhu, G.; Zhu, Y.; Chen, X.; Zhang, Z.; Wang, S.; Yuan, B.; Feng, Y. Facile Preparation of Biocompatible Sulfhydryl Cotton Fiber-Based Sorbents by "Thiol−Ene" Click Chemistry for Biological Analysis. *ACS Appl. Mater. Interfaces* **2014**, *6*, 17857−17864.
(43) Cao, L.; Yu, L.; Guo, Z.; Shen, A.; Guo, Y.; Liang, X. N-Glycosylation Site Analysis of Proteins from Saccharomyces Cerevisiae by Using Hydrophilic Interaction Liquid Chromatography-Based Enrichment, Parallel Deglycosylation, and Mass Spectrometry. *J. Proteome Res.* **2014**, *13*, 1485−1493.
(44) Shen, A.; Li, X.; Dong, X.; Wei, J.; Guo, Z.; Liang, X. Glutathione-Based Zwitterionic Stationary Phase for Hydrophilic Interaction/Cation-Exchange Mixed-Mode Chromatography. *J. Chromatogr. A* **2013**, *1314*, 63−69.

DOI: 10.1021/acsami.6b11572
ACS Appl. Mater. Interfaces 2016, 8, 32060−32067